

Matrix Product States for Quantum Stochastic Modeling

Chengran Yang,^{1, 2, *} Felix C. Binder,^{1, 2, †} Varun Narasimhachar,^{1, 2} and Mile Gu^{1, 2, 3, ‡}

¹*School of Physical and Mathematical Sciences, Nanyang Technological University, 637371 Singapore, Singapore*

²*Complexity institute, Nanyang Technological University, 637335 Singapore, Singapore*

³*Centre for Quantum Technologies, National University of Singapore, 3 Science Drive 2, 117543 Singapore, Singapore*

(Dated: December 3, 2024)

The pursuit of simplicity underlies most of quantitative science. In stochastic modeling, there has been significant effort towards finding models that predict a process' future using minimal information from its past. Meanwhile, in condensed matter physics, finding efficient representations for large quantum many-body systems is a topic of critical concern – exemplified by the development of the matrix product state (MPS) formalism. In this letter, we connect these two distinct fields. Specifically, we associate each stochastic process with a suitable quantum state of a spin-chain. We show that the optimal predictive model for the process leads directly to the MPS representation of the associated quantum state. Conversely, MPS methods offer a systematic construction of q-simulators – the currently best known predictive quantum models for stochastic processes. We show that the memory requirements of these models directly coincide with the bipartite entanglement of an associated spin-chain, providing an analytical connection between quantum correlations in many body physics and the complexity of stochastic modeling.

The quest for simple representations and models of the physical world, often phrased as Ockham's famous razor, underlies most scientific pursuits. This is not only true at the level of the basic theories of physics but equally for the representation of emergent phenomena. Not least, simplicity is also desired at the practical end: using minimal resources to describe complex phenomena.

In condensed matter, simplicity is sought after for the description of quantum many-body systems. Tensor networks such as matrix product states (MPS), for instance, provide an efficient and useful description of one-dimensional quantum systems such as spin-chains [1–3]. This led to reliable and powerful numerical methods for probing and simulating properties of multi-partite systems, whose study would be otherwise intractable [4–7].

The quest for simplicity is equally inherent in computational mechanics, which seeks the most memory-efficient predictive models of complex stochastic processes [8–10]. The classically minimal models, ε -machines, have been used in diverse contexts, such as neuroscience [11], geomagnetism [12], the stock market [13, 14], crystallography [15–17], spin-chains [18], contextuality [19] and non-equilibrium thermodynamics [20, 21]. Recently, it was shown that quantum extensions of ε -machines could further reduce their memory [22], leading to numerous studies to find the most memory-efficient quantum means of predictive modeling [23–34].

In this letter, we connect the two hitherto distinct, powerful formalisms (see Fig. 1). We associate each stochastic process with a suitable quantum state of a spin-chain, measurement of which generates the corresponding stochastic process. We then show that the classical ε -machine of the process leads to a systematic MPS

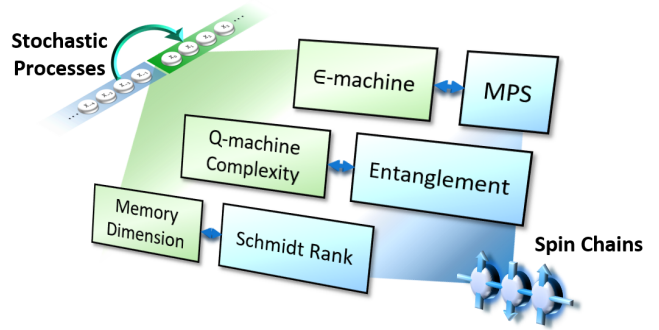


Fig. 1. [color online] This letter connects the complexity of stochastic processes and the representational complexity of spin-chains. These (i) link ε -machines, the provably optimal predictors of a process with the MPS states of a spin-chain, (ii) the memory used to simulate a process quantum mechanically with the entanglement of the spin-chain and (iii) the Hilbert space dimension of such quantum simulators with the Schmidt rank of the spin-chain.

representation of the spin-chain state. Conversely, applying MPS methods to this state allows us to construct a q-simulator for the associated stochastic process – the best known quantum model. Lastly, we show that the entanglement of the aforementioned spin-chain coincides exactly with the memory requirements of the resulting q-simulator. These results provide a direct means of using MPS methods to study the resource requirements of quantum stochastic simulation, extending their relevance to the field of predictive modeling.

Predictive models – A stochastic process is a bi-infinite sequence of random variables $\overleftrightarrow{X} := \cdots X_{-1} X_0 X_1 \cdots$ where each X_t takes values x_t from some finite alphabet \mathcal{A} . Such a process ‘emits’ infinite sequences $\overleftrightarrow{x} := \cdots x_{-1} x_0 x_1 \cdots$ with probability $P(\overleftrightarrow{x})$. We denote $x_{t:t+L} := x_t x_{t+1} \cdots x_{t+L-1}$ and

* Yangchengran92@gmail.com

† quantum@felix-binder.net

‡ mgu@quantumcomplexity.org

$X_{t:t+L} := X_t X_{t+1} \cdots X_{t+L-1}$. Here, we assume the process to be *stationary*, such that $P(X_{t:t+L}) = P(X_{0:L})$ for all t and $L \geq 1$. Hence, we may choose $t = 0$ as the present and omit the subscript t .

Each instance of a process has a particular past, $\overleftarrow{x} := x_{-\infty:0}$, with corresponding conditional future $P(\overrightarrow{X}|\overleftarrow{x})$. Computational mechanics is concerned with building the simplest predictive models that, when given sufficient information about the past $\overleftarrow{x} := x_{-\infty:0}$, can generate future predictions which are statistically indistinguishable from the process itself. That is, the model should generate random variables $\overrightarrow{X} := X_{0:\infty}$ governed by the conditional probability distribution $P(\overrightarrow{X}|\overleftarrow{x})$.

Storing past information, however, costs resources. There is thus interest in generating statistically correct predictions using minimal past information. In this context, storing the entire past is generally wasteful. For instance, when modeling a Markovian process, storing the very last output suffices; anything more would be redundant. In this spirit, computational mechanics groups pasts with identical future statistics into equivalence classes called *causal states* (labeled s_i) by the equivalence relation

$$\overleftarrow{x} \sim_{\varepsilon} \overleftarrow{x}' \text{ iff } P(\overrightarrow{X}|\overleftarrow{x}) = P(\overrightarrow{X}|\overleftarrow{x}'). \quad (1)$$

The resulting model, called ε -machine, generates correct future predictions by tracking only which causal state s_i the past is in. At each time step, it generates an output x according to a set of transition probabilities $T_{kj}^x := P(x, s_j|s_k)$ (transitioning from causal state s_k to s_j). An ε -machine is a provably memory-minimal predictive model for a given process [9].

As reflected in its name, a process' stationary distribution π_k of being in causal state s_k is invariant under time-translation. Furthermore, a process is *irreducible and ergodic* if any distribution of causal states converges to the stationary distribution after infinitely many transition steps.

We may understand the minimal amount of memory that a predictive model requires about the past as the inherent structural complexity of the corresponding process. Any Renyi entropy of the stationary distribution may serve as its quantifier:

$$C_{\mu}^{\alpha} := \frac{1}{1-\alpha} \log_2 \left(\sum_k \pi_k^{\alpha} \right). \quad (2)$$

There are two particularly meaningful cases. The most well-studied is the *statistical complexity* $C_{\mu} \equiv C_{\mu}^1$ [8, 35] which quantifies the amount of past information a classical predictive model must retain – as measured by Shannon entropy. Meanwhile, the *topological complexity* C_{μ}^0 [36] represents a single-shot measure of memory cost, capturing the minimal number of configuration states of a predictive model.

Quantum models – Going beyond (classical) ε -machines quantum models allow for further memory reduction [22, 23, 27, 28] – the most memory-efficient model

to date being q-simulator [27, 28]. Instead of storing classical causal states s_k , a q-simulator retains quantum states $|\sigma_k\rangle$ in its working memory – each with probability π_k :

$$\phi := \sum_k \pi_k |\sigma_k\rangle \langle \sigma_k|. \quad (3)$$

There always exists unitary operator U which interacts this memory register with another quantum system in the initial state $|0\rangle$ such that

$$U|\sigma_k\rangle|0\rangle = \sum_{j,x} \sqrt{T_{jk}^x} |\sigma_j\rangle|x\rangle. \quad (4)$$

Here, $|x\rangle$ forms an orthonormal basis, in one-to-one correspondence to the elements of the alphabet \mathcal{A} . Measurement of the output system in the basis $|x\rangle$ generates the output x with probability T_{jk}^x as desired, collapsing the memory system into the corresponding quantum state $|\sigma_j\rangle$ in the process. Repeated iteration of unitary interaction and measurement generates an output which is statistically identical to the original stochastic process. Due to stationarity the memory register remains in state ϕ after each transition [28]. The amount of required quantum memory may be quantified by the quantum Renyi entropy:

$$C_q^{\alpha} := \frac{1}{1-\alpha} \log_2 (Tr[\phi^{\alpha}]). \quad (5)$$

Analogous to the classical case, $C_q \equiv C_q^1$ represents the average entropic memory required by the q-simulator and we refer to it as the *quantum machine complexity*. C_q^0 quantifies the dimension of the memory Hilbert space $\mathcal{H}_m := \text{span}\{|\sigma_j\rangle\}$. Importantly, such quantum encoding almost always leads to a reduction in entropic memory cost ($C_q^1 \leq C_{\mu}^1$). Select processes where q-simulators use fewer dimensions ($C_q^0 \leq C_{\mu}^0$) have also been recently identified, though general conditions of when this occurs remains an open question [37].

Matrix Product States – Consider a translationally invariant quantum state of a 1D spin-chain with N sites, expressed as

$$|\psi\rangle = \sum_{x_1 x_2 \cdots x_N} c_{x_1 x_2 \cdots x_N} |x_1 x_2 \cdots x_N\rangle, \quad (6)$$

where $\{|x_s\rangle\}$ is an orthonormal basis of each local Hilbert space. Such a description in terms of coefficients $c_{x_1 x_2 \cdots x_N}$ grows exponentially with N . MPSs [38, 39] mitigate this adverse scaling by expressing

$$c_{x_1 x_2 \cdots x_N} = \langle b_l | A^{x_1} A^{x_2} \cdots A^{x_N} | b_r \rangle, \quad (7)$$

where each A^{x_s} is an $m \times m$ complex matrix and $\{|b_l\rangle, |b_r\rangle\}$ are the boundaries. This description gives rise to an intuitive graphical representation (Fig. 2).

When $N \rightarrow \infty$, we obtain an infinite MPS (iMPS). Many of its properties are determined by the *transfer*

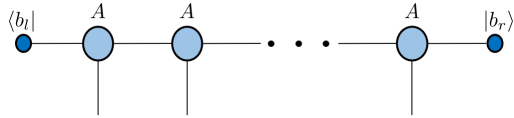


Fig. 2. [color online] Each site matrix A of an MPS is depicted by a node with one ‘leg’ representing each of its indices. A link between two nodes indicates summation over the corresponding index.

matrix \mathbb{E} (see Fig. 3)

$$\mathbb{E} = \sum_x A^x \otimes (A^x)^* \quad (8)$$

where $(A^x)^*$ is the complex conjugate of A^x . If the largest-magnitude eigenvalue η of \mathbb{E} is non-degenerate, the boundary becomes irrelevant [38, 39]. This is because after applying infinitely many transfer matrices to any potential boundary, it converges to the domain left and right eigenvectors of \mathbb{E} , V_l and V_r – i.e., $\langle b_l | \langle b_l |^* \mathbb{E}^\infty \sim V_l$ and $\mathbb{E}^\infty | b_r \rangle | b_r \rangle^* \sim V_r$. Note that each domain eigenvector shown in Fig 3 has two legs. If we designate one index as row index and the other as column index, the domain eigenvectors become matrices, i.e. V_l and V_r (see Supplementary Information A).

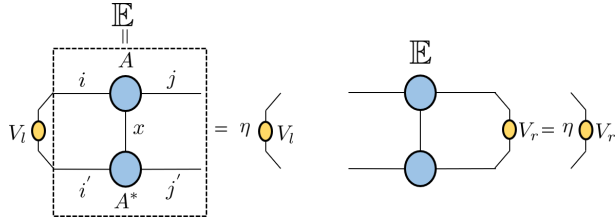


Fig. 3. [color online] The transfer matrix \mathbb{E} has a largest eigenvalue η . The corresponding left and right eigenvectors, V_l and V_r , are $m \times m$ -matrices.

Predictive models and MPS representation – Here we present our main results – the connection between predictive models and the MPS formalism. This is done by associating a stochastic process with a large entangled 1D quantum state

$$|P(\overleftrightarrow{x})\rangle = \sum_{\overleftrightarrow{x}} \sqrt{P(\overleftrightarrow{x})} |\overleftrightarrow{x}\rangle, \quad (9)$$

where $|\overleftrightarrow{x}\rangle$ is an orthonormal basis corresponding to the outputs \overleftrightarrow{x} . Measuring the quantum state in the basis $|\overleftrightarrow{x}\rangle$ generates the stochastic process. $|P(\overleftrightarrow{x})\rangle$ are known as *q-samples* [40, 41], and lie at the heart of many quantum sampling problems [42–46].

Here, we consider q-samples of irreducible, ergodic and stationary stochastic processes \overleftrightarrow{X} . Our first result relates the q-sample representation of such processes to their corresponding ε -machines.

Theorem 1. *A stochastic process \overleftrightarrow{X} , represented by an ε -machine with transition matrix T , is fully represented*

by the iMPS with site matrix

$$A_{kj}^x = \sqrt{T_{kj}^x}. \quad (10)$$

Proof. First, we construct a finite quantum state

$$|\psi\rangle = \sum_{x:t:t+L} \langle 0 | A^{x_t} A^{x_{t+1}} \dots A^{x_{t+L-1}} | 0 \rangle | x_{t:t+L} \rangle \quad (11)$$

with a boundary $|0\rangle$. In the limit $L \rightarrow \infty, t \rightarrow -\infty$, this yields the iMPS. Since each element of each A^x is non-negative the amplitudes generated by the iMPS are as well. In Supplementary Information B we prove that the largest-magnitude eigenvalue of the transfer matrix of the iMPS given by Eq. (10) is non-degenerate if and only if the process is irreducible and ergodic. Hence, the boundary is irrelevant.

Thus, we only need to show that the amplitudes correspond to the classical distribution $P(\overleftrightarrow{X})$. In Supplementary Information A, the probability distribution generated by the iMPS is shown to be

$$\begin{aligned} P_{\text{MPS}}(X_{t:t+L} = x_{t:t+L}) = \\ \text{Tr}(A^{x_{t+L-1}\dagger} \dots A^{x_t\dagger} V_l A^{x_t} \dots A^{x_{t+L-1}} V_r). \end{aligned} \quad (12)$$

The domain left eigenvector V_l and domain right eigenvector V_r have the following form

$$V_l = \sum_k \pi_k |k\rangle \langle k| \quad V_r = \sum_{k,j} \langle \sigma_k | \sigma_j \rangle |k\rangle \langle j| \quad (13)$$

where π_k are the stationary probabilities of causal states s_k and $|j\rangle$ is an orthonormal local site basis (See Supplementary Information C). $|\sigma_k\rangle$ are the internal states of the corresponding q-simulator in Eq. (4). Inserting these expressions into Eq. (12), we obtain

$$P_{\text{MPS}}(X_{t:t+L}) = P(X_{t:t+L}), \quad (14)$$

as shown in Supplementary Information D in more detail. In the limit $L \rightarrow \infty, t \rightarrow -\infty$, this distribution becomes $P(\overleftrightarrow{X})$. \square

This theorem demonstrates that a classical ε -machine of a stochastic process gives direct rise to an iMPS. This representation has a clear operational meaning: each element of the site matrix corresponds to the transition probability between classical causal states. Therefore, it allows for the interpretation of many-body condensed matter systems from the perspective of classical ε -machines.

Now, we make use of this MPS representation to point out the relation between the quantum machine complexity and the entanglement of a process’ q-sample across any bi-partition.

Theorem 2. *The entanglement across any bi-partition of a stochastic process’ q-sample equals the quantum machine complexity C_q . Its Schmidt rank is equal to the dimension of the memory Hilbert space.*

Proof. First, the domain left and right eigenvectors can always be decomposed as $V_l = W_l^\dagger W_l$ and $V_r = W_r W_r^\dagger$. The Schmidt coefficients are the positive square roots of the eigenvalues of the density matrix $\rho = W_l W_r W_r^\dagger W_l^\dagger = W_l V_r W_l^\dagger$ (see Supplementary Information A). In line with Eq. (13) we choose $W_l = \sum_k \sqrt{\pi_k} |k\rangle\langle k|$. Then we construct a quantum state

$$|\psi_{AB}\rangle = \sum_k \sqrt{\pi_k} |k\rangle_A |\sigma_k\rangle_B^* \quad (15)$$

where $|\sigma_k\rangle^*$ is the complex conjugate of $|\sigma_k\rangle$. Partial trace over system B yields

$$\rho_A = \sum_{k,j} \sqrt{\pi_k \pi_j} \langle \sigma_k | \sigma_j \rangle |k\rangle\langle j| = W_l V_r W_l^\dagger \quad (16)$$

Thus, the Schmidt coefficients of the q-sample are the square roots of the density matrix ρ_A 's eigenvalues (see Supplementary Information A). On the other hand, partial trace over system A gives

$$\rho_B = \sum_k \pi_k |\sigma_k\rangle^* \langle \sigma_k|^*. \quad (17)$$

Note that the complex conjugate of ρ_B is equal to ϕ (Eq. 3). Hence, since ρ_A and ρ_B must have the same spectrum, ρ_A also has the same spectrum as ϕ . Thus, the Schmidt coefficients are the square roots of the eigenvalues of ϕ .

This implies that any Renyi entropy of the squared Schmidt coefficients and the corresponding entropy of ϕ are also equal

$$H_\alpha(c_k^2) = H_\alpha(\phi) \quad (18)$$

For the special cases $\alpha = 1$ and $\alpha = 0$, we obtain Theorem 2. \square

This result entails a novel method for computing C_q , by calculating the bi-partite entanglement E of the underlying process' q-sample in terms of the Schmidt coefficients. Furthermore, the Schmidt rank corresponds to the dimension of the memory Hilbert space. Conversely, C_q^0 bounds the logarithm of the minimal dimension needed for generating $|p(\overrightarrow{x})\rangle$. In fact, the dimension of the q-simulator's memory is equal to the rank of the domain right eigenvector V_r .

Corollary 1. *A process can be modeled using a quantum system of fewer dimensions than the provably optimal classical counterpart whenever domain right eigenvector V_r is not full rank.*

This corollary provides an efficient way to identify whether the internal quantum states can be encoded into a smaller Hilbert space. Thus, this opens the potential for the use of MPS methods to isolate the exact conditions for which C_q^0 is strictly less than the number of causal states.

Our final result presents a systematic means of constructing stochastic process' q-simulator from the MPS of its q-sample. In particular, the domain eigenvectors can be employed to immediately ascertain the internal memory states $|\sigma_j\rangle$ of q-simulator, and its associated unitary operation. The proof is included in Supplementary Information E.

Theorem 3. *The q-simulator for a stochastic process [28] can be systematically constructed from its iMPS representation according to Theorem 1:*

1. *The internal quantum states of the q-simulator are*

$$|\sigma_j\rangle := W_r^\dagger |j\rangle \quad (19)$$

where W_r is a decomposition $W_r W_r^\dagger = V_r$ such that the image of W_r^\dagger is the same as the image of V_r .

2. *The stepwise unitary interaction of the q-simulator is given by*

$$\langle x|U|0\rangle := (W_r^{-1} A^x W_r)^\dagger, \quad (20)$$

where W_r^{-1} is defined to be the inverse matrix of W_r on the memory Hilbert space $\mathcal{H}_m = \text{span}\{|\sigma_k\rangle\}$.

Nemo Process – We illustrate these results using the Nemo process [27], as defined by its ϵ -machine in Fig. 4. This process has infinite Markov order – i.e., regardless of how many past outputs one has observed, observing one more output will always further improve the capacity to predict the future. This property made such processes challenging to model prior to the development of computational mechanics.

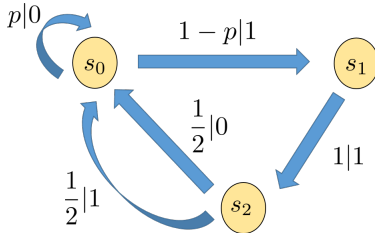


Fig. 4. [color online] The Nemo process is defined for $0 < p < 1$ and has causal states s_1 , s_2 , and s_3 . An edge from s_i to s_j indicates a non-zero transition probability, labelled ' $P(x, s_j | s_i)x$ '.

Consider the Nemo process' statistics $P(\overleftarrow{X}, \overrightarrow{X})$ and its q-sample $|\psi\rangle$. Our results allow (1) direct construction of an MPS representation for $|\psi\rangle$, (2) the use of MPS methods to find the q-simulator for the Nemo process, and (3) evaluation the corresponding quantum advantage of simulating such a process quantum mechanically. First, according to Theorem 1, the iMPS site matrix for $|\psi\rangle$ is given by

$$A^0 = \begin{bmatrix} \sqrt{p} & 0 & 0 \\ 0 & 0 & 0 \\ \frac{1}{\sqrt{2}} & 0 & 0 \end{bmatrix} \quad A^1 = \begin{bmatrix} 0 & \sqrt{1-p} & 0 \\ 0 & 0 & 1 \\ \frac{1}{\sqrt{2}} & 0 & 0 \end{bmatrix} \quad (21)$$

Using Theorem 2 and Corollary 1, we can compute the quantum memory C_q by using the MPS to quantify the entanglement in $|\psi\rangle$. C_q is plotted, along with C_μ , in Fig. 5. Clearly, the q -simulator require less memory than provably optimal counterparts for all allowed values p .

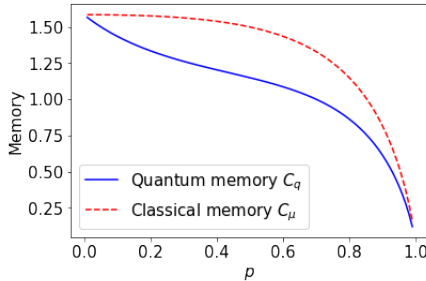


Fig. 5. [color online] The amount of quantum memory C_q required for simulating the Nemo process is less than the classical memory C_μ for all $0 < p < 1$.

The internal quantum states and the unitary operator U are also straightforward to obtain, by virtue of Theorem 3 (see Supplementary Information F).

Conclusion – We have connected two previously distinct notions of complexity: the memory cost of prediction and the representational complexity of spin-chains – allowing results in one field to catalyze new insights in the other. By associating each stochastic process with a suitable quantum state of a spin-chain, we demonstrated that predictive models constructed in complexity science lead directly to the MPS representation of the general classical stochastic process. Conversely, optimization using standard MPS techniques allows systematic construction of q -simulators – the current state of the art for predictive modeling. Moreover, we established that the memory re-

quirement of such q -simulators exactly coincides with the bipartite entanglement in the associated spin-chain state.

These results open a number of promising avenues for future research. First, we observe that the associated spin-chain state of a stochastic process is in fact a quantum superposition over all realizations of the process. Such states, known as q -samples, are associated with quantum computational speed-up, as seen in boson sampling [42–46] and the graph-isomorphism problem [40]. Our q -simulators offers a means of generating such states efficiently. Meanwhile, the proven equivalence between memory dimension and Schmidt rank offers a first systematic means to identify processes where quantum simulators show advantage in single-shot scenarios. Finally, tensor networks offer sophisticated techniques to reduce the bond dimension of represented processes at the cost of introducing small inaccuracies. Such methods can now be adapted to quantum modeling – allowing the construction of approximate models with drastically reduced dimensional requirements. Our approach complements other uses of tensor network methods for the description of classical systems with stochastic elements [47–53] and other works that sample stochastic processes by measuring a suitable quantum state in a predefined basis [40, 42].

ACKNOWLEDGMENTS

The authors thank J. Thompson, D. Poletti, I. Arad, J. Mahoney, J. Crutchfield, and T. Elliott for useful discussions. This work was supported by the National Research Foundation of Singapore (Fellowship NRF-NRFF2016-02), the John Templeton Foundation (grant 53914), the FQXi Large Grant: Physics of the Observer.

[1] I. Affleck, T. Kennedy, E. H. Lieb, and H. Tasaki, Physical Review Letters **59**, 799 (1987).

[2] A. Klümper, A. Schadschneider, and J. Zittartz, Epl **24**, 293 (1993), arXiv:9307028 [cond-mat].

[3] T. Prosen, Physical Review Letters **106**, 217206 (2011), arXiv:1103.1350.

[4] S. R. White, Physical Review Letters **69**, 2863 (1992).

[5] F. Verstraete, D. Porras, and J. I. Cirac, Physical Review Letters **93**, 227205 (2004), arXiv:0404706 [cond-mat].

[6] G. Vidal, Physical Review Letters **99**, 220405 (2007), arXiv:0512165 [cond-mat].

[7] R. Orús and G. Vidal, Physical Review B - Condensed Matter and Materials Physics **78**, 155117 (2008), arXiv:0711.3960.

[8] J. P. Crutchfield and K. Young, Physical Review Letters **63**, 105 (1989).

[9] C. R. Shalizi and J. P. Crutchfield, Journal of Statistical Physics **104**, 817 (2001), arXiv:9907176 [cond-mat].

[10] J. P. Crutchfield, Nature Physics **8**, 17 (2012).

[11] R. Haslinger, K. L. Klinkner, and C. R. Shalizi, Neural Computation **22**, 121 (2010), arXiv:1001.0036.

[12] R. W. Clarke, M. P. Freeman, and N. W. Watkins, Physical Review E **67**, 016203 (2003).

[13] J. S. Yang, W. Kwak, T. Kaizoji, and I. M. Kim, European Physical Journal B **61**, 241 (2008), arXiv:0701179 [physics].

[14] J. B. Park, J. Won Lee, J. S. Yang, H. H. Jo, and H. T. Moon, Physica A: Statistical Mechanics and its Applications **379**, 179 (2007).

[15] D. P. Varn, G. S. Canright, and J. P. Crutchfield, Physical Review B - Condensed Matter and Materials Physics **66**, 174110 (2002), arXiv:0203290 [cond-mat].

[16] D. P. Varn, G. S. Canright, and J. P. Crutchfield, Acta Crystallographica Section A: Foundations of Crystallography **69**, 197 (2013).

[17] D. P. Varn and J. P. Crutchfield, Current Opinion in Chemical Engineering **7**, 47 (2015), arXiv:1409.5930.

[18] D. P. Feldman and J. P. Crutchfield, Physics Letters A **238**, 244 (1998), arXiv:9708186 [cond-mat].

[19] A. Cabello, M. Gu, O. Gühne, and Z.-P. Xu, arXiv preprint arXiv:1709.07372 (2017).

[20] A. B. Boyd, D. Mandal, and J. P. Crutchfield, *New Journal of Physics* **18**, 023049 (2015), arXiv:1507.01537.

[21] A. J. Garner, J. Thompson, V. Vedral, and M. Gu, *Physical Review E* **95**, 042140 (2017), arXiv:1510.00010.

[22] M. Gu, K. Wiesner, E. Rieper, and V. Vedral, *Nature Communications* **3**, 762 (2012), arXiv:arXiv:1102.1994v5.

[23] P. M. Riechers, J. R. Mahoney, C. Aghamohammadi, and J. P. Crutchfield, *Physical Review A* **93**, 052317 (2016), arXiv:1510.08186.

[24] W. Y. Suen, J. Thompson, A. J. P. Garner, V. Vedral, and M. Gu, *Quantum* **1**, 25 (2017), arXiv:1511.05738.

[25] C. Aghamohammadi, J. R. Mahoney, and J. P. Crutchfield, *Physics Letters, Section A: General, Atomic and Solid State Physics* **381**, 1223 (2017).

[26] C. Aghamohammadi, J. R. Mahoney, and J. P. Crutchfield, *Scientific Reports* **7**, 6735 (2017), arXiv:1609.03650.

[27] J. R. Mahoney, C. Aghamohammadi, and J. P. Crutchfield, *Scientific Reports* **6**, 20495 (2016), arXiv:1508.02760.

[28] F. C. Binder, J. Thompson, and M. Gu, arXiv preprint (2017), arXiv:1709.02375.

[29] C. Aghamohammadi, S. P. Loomis, J. R. Mahoney, and J. P. Crutchfield, *Physical Review X* **8**, 011025 (2018), arXiv:1707.09553.

[30] T. J. Elliott and M. Gu, *npj Quantum Information* **4**, 18 (2018).

[31] M. S. Palsson, M. Gu, J. Ho, H. M. Wiseman, and G. J. Pryde, *Science Advances* **3**, e1601302 (2017), arXiv:1602.05683.

[32] A. J. P. Garner, Q. Liu, J. Thompson, V. Vedral, and M. Gu, *New Journal of Physics* **19**, 103009 (2016), arXiv:1609.04408.

[33] F. G. Jouneghani, M. Gu, J. Ho, J. Thompson, W. Y. Suen, H. M. Wiseman, and G. J. Pryde, arXiv preprint (2017), arXiv:1711.03661.

[34] T. J. Elliott, A. J. P. Garner, and M. Gu, arXiv preprint, 1803.05426 (2018).

[35] N. Perry and P. M. Binder, *Physical Review E - Statistical Physics, Plasmas, Fluids, and Related Interdisciplinary Topics* **60**, 459 (1999).

[36] J. P. Crutchfield, *Inside versus Outside* **63**, 235 (1994).

[37] J. Thompson, A. J. P. Garner, J. R. Mahoney, J. P. Crutchfield, V. Vedral, and M. Gu, arXiv preprint (2017), arXiv:1712.02368.

[38] U. Schollwöck, *Annals of Physics* **326**, 96 (2011), arXiv:1008.3477.

[39] R. Orús, *Annals of Physics* **349**, 117 (2014), arXiv:1306.2164.

[40] D. Aharonov and A. Ta-Shma, in *Proceedings of the thirty-fifth annual ACM symposium on Theory of computing* (2003) p. 20, arXiv:0301023 [quant-ph].

[41] S. Arunachalam and R. de Wolf, arXiv preprint (2016), arXiv:1607.00932.

[42] S. Aaronson and A. Arkhipov, in *Proceedings of the forty-third annual ACM symposium on Theory of computing* (ACM, 2011) p. 333, arXiv:1011.3245.

[43] J. B. Spring, B. J. Metcalf, P. C. Humphreys, W. S. Kolthammer, X. M. Jin, M. Barbieri, A. Datta, N. Thomas-Peter, N. K. Langford, D. Kundys, J. C. Gates, B. J. Smith, P. G. Smith, and I. A. Walmsley, *Science* **339**, 798 (2013), arXiv:1212.2622.

[44] A. Crespi, R. Osellame, R. Ramponi, D. J. Brod, E. F. Galvão, N. Spagnolo, C. Vitelli, E. Maiorino, P. Mataloni, and F. Sciarrino, *Nature Photonics* **7**, 545 (2013).

[45] A. P. Lund, A. Laing, S. Rahimi-Keshari, T. Rudolph, J. L. O'Brien, and T. C. Ralph, *Physical Review Letters* **113**, 100502 (2014), arXiv:1305.4346.

[46] S. Aaronson and L. Chen, arXiv preprint (2016), arXiv:1612.05903.

[47] T. H. Johnson, S. R. Clark, and D. Jaksch, *Physical Review E - Statistical, Nonlinear, and Soft Matter Physics* **82**, 16 (2010), arXiv:1006.2639.

[48] T. H. Johnson, T. J. Elliott, S. R. Clark, and D. Jaksch, *Physical Review Letters* **114**, 090602 (2015), arXiv:1410.3319.

[49] Z.-Y. Han, J. Wang, H. Fan, L. Wang, and P. Zhang, arXiv preprint (2017), arXiv:1709.01662.

[50] A. Novikov, M. Trofimov, and I. Oseledets, arXiv preprint (2016), arXiv:1605.03795.

[51] E. M. Stoudenmire, arXiv preprint (2017), arXiv:1801.00315.

[52] E. M. Stoudenmire and D. J. Schwab, in *Advances in Neural Information Processing Systems* (2016) pp. 4799—4807, arXiv:1605.05775.

[53] H. A. Loeliger and P. O. Vontobel, *IEEE Transactions on Information Theory* **63**, 5642 (2017), arXiv:1508.00689.

SUPPLEMENTARY INFORMATION

Supplementary Information A: MPS and Canonical form

Consider an iMPS $\{A^x\}$ with left and right boundaries $\{\langle b_l |, | b_r \rangle\}$. In order to link the transfer matrix \mathbb{E} of this iMPS to a completely positive (CP) map we introduce the left and right *vec maps* \mathcal{V}_l and \mathcal{V}_r :

$$\mathcal{V}_l : \langle j | \langle i | \rightarrow | i \rangle \langle j | \quad \mathcal{V}_r : | i \rangle | j \rangle \rightarrow | i \rangle \langle j | \quad (S1)$$

A graphical representation of these maps is shown in Fig S1.

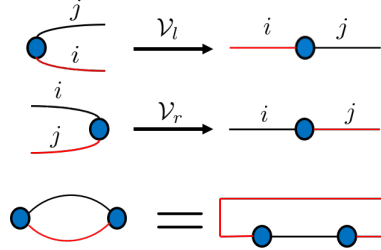


Fig. S1. [color online] In graphical representation, a vec map is the operation which bends the leg of a node to the other side.

Applying the left vec map and right vec map to the transfer matrix gives

$$\begin{aligned} \mathcal{E}_l(|j\rangle\langle i|) &:= \mathcal{V}_l(\langle j | \langle i | \mathbb{E}) = \sum_x (A^x)^\dagger |i\rangle\langle j| A^x \\ \mathcal{E}_r(|j\rangle\langle i|) &:= \mathcal{V}_r(\mathbb{E}|j\rangle|i\rangle) = \sum_x A^x |j\rangle\langle i| (A^x)^\dagger \end{aligned} \quad (S2)$$

For an iMPS whose transfer matrix' largest-magnitude eigenvalue is unique, the boundary does not affect the expectation value of any local observable \mathcal{O} on a finite interval of N sites. This can be seen from the fact that any boundary converges to the domain eigenvector of the transfer matrix after applying the transfer matrix infinitely many times (see Fig. S2).

$$\langle \mathcal{O} \rangle = \mathbb{B}_l \mathbb{E}^\infty \mathbb{E}_\mathcal{O} \mathbb{E}^\infty \mathbb{B}_r = \mathbb{V}_l \mathbb{E}_\mathcal{O} \mathbb{V}_r \quad (S3)$$

where $\mathbb{E}_\mathcal{O} = \sum_{x_{1:N}, x'_{1:N}} \langle x_{1:N} | \mathcal{O} | x'_{1:N} \rangle (A^{x_1} \cdots A^{x_N}) \otimes (A^{x'_1} \cdots A^{x'_N})^*$ and $\mathbb{B}_l = \langle b_l | \langle b_l |^*, \mathbb{B}_r = | b_r \rangle | b_r \rangle^*$. Thus, different boundaries give the same expectation value of a local observable. In this case, we can ignore the boundary and focus on the site matrices.

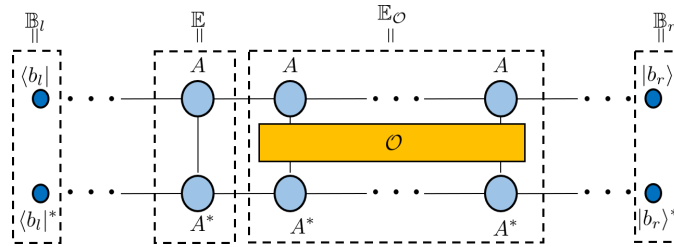


Fig. S2. The graphical representation of expectation value $\langle \mathcal{O} \rangle$. A^* denotes the complex conjugate of A . The block in the middle represents the observable $\mathbb{E}_\mathcal{O}$, which is a multi-index tensor. The blue nodes are the boundary. The expectation value is given by contracting all indices.

As the measurement in the computational basis corresponds to the measurement operators $\mathcal{O} = |x_{t:t+L}\rangle\langle x_{t:t+L}|$ for finite t and L , the distribution of the measurement outcomes is then the expectation value of the measurement operators, i.e.,

$$\begin{aligned} P_{\text{MPS}}(X_{t:t+L} = x_{t:t+L}) &= \mathbb{V}_l \mathbb{E}_\mathcal{O} \mathbb{V}_r \\ &= \text{Tr} [\mathcal{V}_l(\mathbb{V}_r \mathbb{E}_\mathcal{O}) \mathcal{V}_r(\mathbb{V}_r)] \\ &= \text{Tr} \left[A^{x_{t+L-1}} \cdots A^{x_t} V_l A^{x_t} \cdots A^{x_{t+L-1}} V_r \right] \end{aligned} \quad (S4)$$

where $V_l = \mathcal{V}_l(\mathbb{V}_l)$ and $V_r = \mathcal{V}_r(\mathbb{V}_r)$. Note that $\mathbb{V}_l \mathbb{E}_O \mathbb{V}_r = \text{Tr}[\mathcal{V}_l(\mathbb{V}_r \mathbb{E}_O) \mathcal{V}_r(\mathbb{V}_r)]$ is obtained from the fact that $\langle i|j|m\rangle|n\rangle = \text{Tr}[\mathcal{V}_l(\langle i|j|) \mathcal{V}_r(|m\rangle|n\rangle)]$

For any iMPS, a special form, called the canonical form, is expressed as the Schmidt decomposition at any bipartition, see Fig. S3. For an iMPS whose transfer matrix' largest-magnitude eigenvalue is non-degenerate, there is a systematic way of obtaining the canonical form [7].

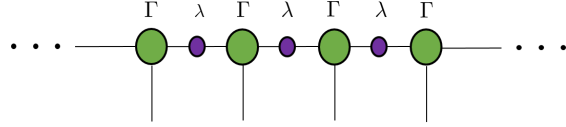


Fig. S3. [color online] The canonical form of an iMPS consists of two types of tensors, both of which are explained in the text. The purple nodes correspond to the Schmidt coefficients.

The essence in computing the canonical form of an iMPS is to deduce its entanglement properties from the transfer matrix \mathbb{E} . This is done in four steps:

- (i) Assume the largest eigenvalue of transfer matrix \mathbb{E} is unique. Find the domain right and left eigenvectors of the transfer matrix \mathbb{E} , V_r and V_l , as shown in Fig. S4. Here, V_l and V_r are rank 2 tensors – i.e., positive Hermitian matrices. Because the transfer matrix \mathbb{E} is not Hermitian, V_l and V_r are generally different from each other.
- (ii) Decompose V_r and V_l separately, $V_r = W_r W_r^\dagger, V_l = W_l^\dagger W_l$, as shown in Fig. S4. For instance, if V_r has the eigenvalue decomposition $V_r = U D U^\dagger$, where U is a unitary matrix and D is a diagonal matrix, then W_r can be set to $W_r = U \sqrt{D}$
- (iii) Insert two identity matrices, $\mathbb{I} = W_r W_r^{-1}$ and $\mathbb{I} = W_l^{-1} W_l$, into the horizontal index, as shown in Fig. S4. Then compute the singular value decomposition of the product $W_l W_r$, namely $W_l W_r = U \lambda V$, where U and V are unitary matrices. λ is a diagonal matrix which contains the Schmidt coefficients of $|\psi\rangle$ across any bipartition of the iMPS.
- (iv) Compute $\Gamma^x = V W_r^{-1} A^x W_l^{-1} U$, as shown in Fig. S4.

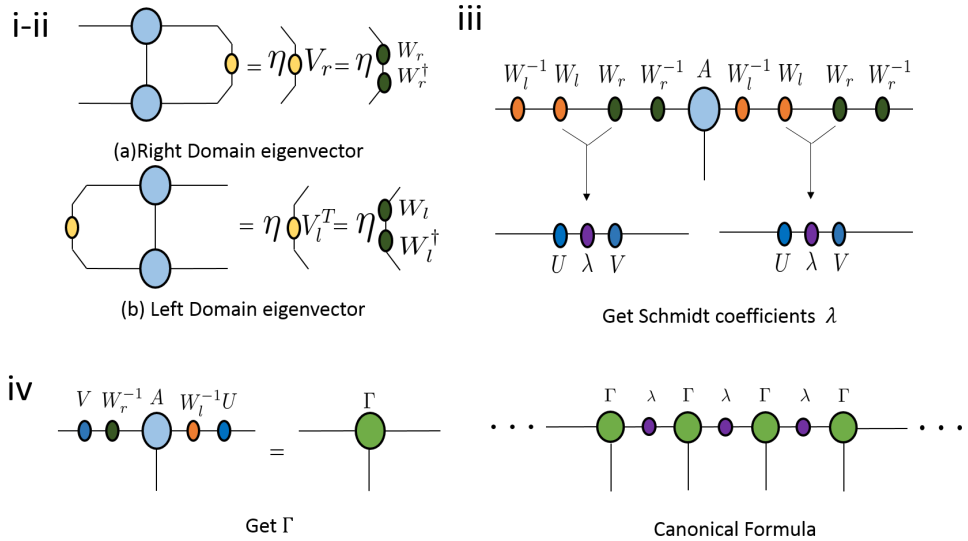


Fig. S4. [Color online] The canonical form $\{\Gamma, \lambda\}$ of Fig. S3 is computed in four steps. λ is obtained in step (iii) as the singular values of $W_l W_r$, whereas Γ is defined in step (iv).

As shown in (iii), the Schmidt coefficients are the singular values of the matrix $W_l W_r$.

Supplementary Information B: The largest eigenvalue of the transfer matrix is unique iff the process is irreducible and ergodic

In this section, we show that the convergence of the transfer matrix of a q-sample's iMPS representation and convergence of the corresponding stochastic process mutually imply each other (Lemma 2, below). We begin with the following intermediate result:

Lemma 1. *The largest eigenvalue of the transfer matrix \mathbb{E} is 1.*

First note that the CP map \mathcal{E}_l given by Eq. S2 has the same eigenvalues as the transfer matrix \mathbb{E} . It hence suffices to show that the largest eigenvalue of \mathcal{E}_l is 1. For the proof we use the matrix norm $\|*\|_1$ which is defined by $\|B\|_1 := \sum_{ij} |B_{ij}|$ for a matrix $B = \sum_{i,j} b_{ij} |i\rangle\langle j|$ in an orthonormal basis $\{|i\rangle\}$. For any rank-1 matrix $|j\rangle\langle k|$,

$$\begin{aligned} & \|\mathcal{E}_l(|j\rangle\langle k|)\|_1 \\ &= \sum_{mn} |\langle m|\mathcal{E}_l(|j\rangle\langle k|)|n\rangle| \\ &= \sum_{mn} \sum_x \sqrt{P(x, s_m|s_j)P(x, s_n|s_k)} \end{aligned} \tag{S5}$$

Since the causal state at the next step is determined by the output symbol and the previous causal state, we obtain

$$\begin{aligned} \sum_{mn} \sum_x \sqrt{P(x, s_m|s_j)P(x, s_n|s_k)} &= \sum_x \sqrt{P(x|s_j)P(x|s_k)} \\ &\leq 1 \end{aligned} \tag{S6}$$

The last step follows from the Cauchy-Schwarz inequality. Equality holds iff $k = j$. For any matrix B as above

$$\|\mathcal{E}_l(B)\|_1 \leq \sum_{ij} |b_{ij}| \|\mathcal{E}_l(|i\rangle\langle j|)\|_1 \leq \sum_{ij} |b_{ij}| = \|B\|_1 \tag{S7}$$

Therefore any eigenvalue λ of \mathcal{E}_l is less or equal to 1.

In general, for any diagonal density matrix $\rho_d = \sum p_k |k\rangle\langle k|$

$$\begin{aligned} \mathcal{E}_l(\rho_d) &= \sum_x (A^x)^\dagger \rho_d A^x \\ &= \sum_x (A^x)^\dagger \sum_k p_k |k\rangle\langle k| A^x \\ &= \sum_j \sum_k p_k \sum_x P(x, s_j|s_k) |j\rangle\langle j| \end{aligned} \tag{S8}$$

For the stationary distribution in particular we define

$$V_l = \sum_k \pi_k |k\rangle\langle k| \tag{S9}$$

which has the following property

$$\mathcal{E}_l(V_l) = V_l \tag{S10}$$

This can be seen from Eq. S8 by noting that $\sum_{x,k} P(x, s_j|s_k) \pi_k = \pi_j$ due to stationarity. In other words, V_l is an eigenvector of \mathcal{E}_l with eigenvalue 1 – hence, a domain eigenvector. \square

Lemma 2. *The transfer matrix has only one eigenvalue, of magnitude one, iff the corresponding process is irreducible and ergodic.*

First, we assume that the process is irreducible and ergodic and that V_l is a domain eigenvector of \mathcal{E}_l . Assume that V_l has non-zero off-diagonal elements. Since $\|\mathcal{E}_l(|j\rangle\langle k|)\|_1 < 1$ for all $j \neq k$,

$$\|\mathcal{E}_l(V_l)\|_1 \leq \sum_{jk} |(V_l)_{jk}| \|\mathcal{E}_l(|j\rangle\langle k|)\|_1 < \|V_l\|_1 \tag{S11}$$

which contradicts $\|\mathcal{E}_l(V_l)\|_1 = \|V_l\|_1$. Thus, V_l only has non-zero diagonal elements. Convergence of the process then ensures that there is only one diagonal matrix that is the domain eigenvector of the CP map \mathcal{E}_l .

The inverse case is also true. We consider again Eq. S8. Assuming that the transfer matrix's largest-magnitude eigenvalue is unique, ρ_d always converges to the matrix $\sum_k \pi_k |k\rangle\langle k|$. Hence, any distribution under transition converges to the stationary distribution. \square

Supplementary Information C: The structure of domain left and right eigenvectors

We show that the domain left and right eigenvectors have the following expressions

$$V_l = \sum_k \pi_k |k\rangle\langle k| \quad (\text{S12})$$

$$V_r = \sum_{k,j} \langle \sigma_k | \sigma_j \rangle |k\rangle\langle j| \quad (\text{S13})$$

As mentioned in Supplementary Information B, the domain left eigenvector is

$$V_l = \sum_k \pi_k |k\rangle\langle k| \quad (\text{S14})$$

For the domain right eigenvector, we show that V_r (Eq. S13) is a fixed point of the CP map $\mathcal{E}_r(\rho) = \sum_x A^x \rho (A^x)^\dagger$. Applying \mathcal{E}_r to V_r , we obtain

$$\begin{aligned} \langle k | \mathcal{E}_r(V_r) | j \rangle &= \sum_x \langle k | A^x V_r A^{x\dagger} | j \rangle \\ &= \sum_{m,n,x} \sqrt{T_{km}^x T_{jn}^x} \langle \sigma_m | \sigma_n \rangle \end{aligned} \quad (\text{S15})$$

Now we use the fact that $U|\sigma_k\rangle|0\rangle = \sum_x \sqrt{T_{km}^x} |\sigma_m\rangle|x\rangle$, which results in

$$\langle \sigma_k | \sigma_j \rangle = \sum_{m,n,x} \sqrt{T_{km}^x T_{jn}^x} \langle \sigma_m | \sigma_n \rangle \quad (\text{S16})$$

Thus, $\langle k | \mathcal{E}_r(V_r) | j \rangle = \langle \sigma_k | \sigma_j \rangle$. In other words, V_r is the domain right eigenvector.

Supplementary Information D: iMPS generates the correct distribution

Here, we prove that the iMPS generates the correct distribution. As shown in Supplementary Information A, the distribution of measurement outcomes of an iMPS is

$$\begin{aligned} P_{MPS}(x_{t:L}) &= \text{Tr}(A^{x_{t+L-1}\dagger} \dots A^{x_t\dagger} V_l A^{x_t} \dots A^{x_{t+L-1}} V_r) \\ &= \sum_n \langle n | A^{x_{t+L-1}\dagger} \dots A^{x_t\dagger} V_l A^{x_t} \dots A^{x_{t+L-1}} \sum_m |m\rangle\langle m| V_r |n\rangle \\ &= \sum_{n,m,i} \pi_j \sqrt{P(x_{t:t+L}, s_n | s_i) P(x_{t:t+L}, s_m | s_i)} \langle \sigma_m | \sigma_n \rangle \end{aligned} \quad (\text{S17})$$

where we have used Eq. S12 and Eq. S13. We note that the next causal state is identified by the output symbol x and the previous causal state. In other words, there exists only one causal state s_n for which $P(x_{t:t+L}, s_n | s_i)$ is non-zero.

$$\begin{aligned} P_{MPS}(x_{t:L}) &= \sum_{i,n} \pi_j P(x_{t:t+L}, s_n | s_i) \langle \sigma_n | \sigma_n \rangle \\ &= P(x_{t:t+L}) \end{aligned} \quad (\text{S18})$$

Supplementary Information E: Proof of Theorem 3

There are two aspects of Theorem 3. First, U defined in Eq. 20 is a unitary operator. More importantly, U couples the quantum signal states with the ancillary system such that correct statistics are generated, i.e., $U|\sigma_k\rangle|0\rangle = \sum_{x,j} \sqrt{T_{kj}^x} |\sigma_j\rangle|x\rangle$.

For the first part, as U is partly defined on the space $\mathcal{H}_m \otimes |0\rangle$, we show that U is an isometry which can be extended to a unitary operator.

Lemma 3. U in Eq. 4 is an isometry such that

$$\begin{aligned} \langle 0|U^\dagger U|0\rangle &= \sum_x W_r^{-1} A^x V_r (A^x)^\dagger (W_r^{-1})^\dagger \\ &= W_r^{-1} V_r (W_r^{-1})^\dagger \\ &= I \end{aligned} \tag{S19}$$

where I is the identity matrix. \square

Before showing that U correctly couples the quantum signal states and the ancillary system, we state two lemmata that discuss the image of the operators A^x and W_r .

Lemma 4. A^x maps a quantum state in memory Hilbert \mathcal{H}_m space to memory Hilbert space, i.e. $A^x|\psi\rangle \in \mathcal{H}_m$ if $|\psi\rangle \in \mathcal{H}_m$.

Assume the domain right eigenvector has the eigenvalue decomposition

$$V_r = \sum_k \lambda_k |\nu_k\rangle\langle\nu_k| \tag{S20}$$

where all λ_k are positive eigenvalues and $|\nu_k\rangle$ is the eigenvector. Assume the lemma is wrong. This implies that there exists a quantum state $|\psi\rangle$ that is not in the memory Hilbert space but satisfies

$$\langle\psi|A^x|\nu_s\rangle \neq 0 \tag{S21}$$

for some $|\nu_s\rangle$ since the basis $|\nu_k\rangle$ spans the memory Hilbert space. Hence

$$\begin{aligned} \langle\psi|V_r|\psi\rangle &= \langle\psi| \sum_x A^x V_r (A^x)^\dagger |\psi\rangle \\ &= \sum_{x,s} \lambda_s |\langle\psi|A^x|\nu_s\rangle|^2 \\ &\geq \lambda_s |\langle\psi|A^x|\nu_s\rangle|^2 \\ &> 0 \end{aligned} \tag{S22}$$

However, $\langle\psi|V_r|\psi\rangle = 0$ contradicts the above equation. Thus, the lemma is correct. \square

Then, we prove that

Lemma 5. W_r maps any quantum state into the memory Hilbert space.

W_r has the singular value decomposition

$$W_r = \sum_i c_i |u_i\rangle\langle v_i| \tag{S23}$$

where c_i is the singular value. $\{|u_i\rangle\}$ and $\{|\langle v_i|\}$ are orthogonal bases. $\{|u_i\rangle\}$ spans the image space of W_r . Thus $V_r = \sum_i c_i^2 |u_i\rangle\langle u_i|$ has the same image space as W_r . And the memory Hilbert space, which is the image of map V_r , is equal to the image of W_r . \square

Combining Lemma 4 and Lemma 5, we have

$$\mathcal{P}_{\mathcal{H}_m} A^x W_r = A^x W_r \tag{S24}$$

where $P_{\mathcal{H}_m}$ is a projector onto the memory Hilbert space \mathcal{H}_m .

Applying U on the quantum state and the ancillary system, we have

$$\begin{aligned}
 U|\sigma_k\rangle|0\rangle &= \sum_x (W_r^{-1} A^x W_r)^\dagger |\sigma_k\rangle|x\rangle \\
 &= \sum_x (P_{\mathcal{H}_m} A^x W_r)^\dagger |k\rangle|x\rangle \\
 &= \sum_{x,j} \sqrt{T_{kj}^x} |\sigma_j\rangle|x\rangle
 \end{aligned} \tag{S25}$$

□

Supplementary Information F: Nemo process

In this section we explicitly derive the quantum signal states $|\sigma_j\rangle$ and the unitary operator U for the Nemo process. They are obtained by operating W_r^\dagger on the basis $|j\rangle$

$$\begin{aligned}
 |\sigma_0\rangle &= c \left(\sqrt{2p} |e_0\rangle + \sqrt{1-p} |e_1\rangle \right) \\
 |\sigma_1\rangle &= c (\sqrt{p} |e_1\rangle + |e_2\rangle) \\
 |\sigma_2\rangle &= c (|e_0\rangle + \sqrt{p} |e_2\rangle)
 \end{aligned} \tag{S26}$$

with $c \equiv (1+p)^{-\frac{1}{2}}$.

According to Theorem 3, the unitary operator U is characterized by

$$\begin{aligned}
 |e_0\rangle|0\rangle &\rightarrow \sqrt{p} |e_0\rangle|0\rangle + \xi |e_1\rangle|0\rangle + \xi |e_1\rangle|1\rangle \\
 |e_1\rangle|0\rangle &\rightarrow |e_2\rangle|1\rangle \\
 |e_2\rangle|0\rangle &\rightarrow |e_0\rangle|1\rangle
 \end{aligned} \tag{S27}$$

where $\xi = \sqrt{\frac{1-p}{2}}$.

The matrix form of U , written in the basis $\{|e_0\rangle|0\rangle, |e_0\rangle|1\rangle, |e_1\rangle|0\rangle, |e_1\rangle|1\rangle, |e_2\rangle|0\rangle, |e_2\rangle|1\rangle\}$ is

$$\begin{bmatrix} \sqrt{p} & \# & 0 & \# & 0 & \# \\ 0 & \# & 0 & \# & 1 & \# \\ \sqrt{\frac{1-p}{2}} & \# & 0 & \# & 0 & \# \\ \sqrt{\frac{1-p}{2}} & \# & 0 & \# & 0 & \# \\ 0 & \# & 0 & \# & 0 & \# \\ 0 & \# & 1 & \# & 0 & \# \end{bmatrix} \tag{S28}$$

where $\#$ denotes undetermined terms which may be assigned by a Gram-Schmidt procedure for the matrix columns.